# I-Motif-Programmed Functionalization of DNA Nanocircles

Tao Li and Michael Famulok*

Life and Medical Science (LIMES) Institute, Program Unit Chemical Biology and Medicinal Chemistry, University of Bonn, 53121 Bonn, Germany

S Supporting Information

ABSTRACT: The folding of various intra- and intermolecular i-motif DNAs is systematically studied to expand the toolbox for the control of mechanical operations in DNA nanoarchitectures. We analyzed i-motif DNAs with two C-tracts under acidic conditions by gel electrophoresis, circular dichroism, and thermal denaturation and show that their intra- versus intermolecular folding primarily depends on the length of the C-tracts. Two stretches of six or fewer C-residues favor the intermolecular folding of i-motifs, whereas longer C-tracts promote the formation of intramolecular i-motif structures with unusually high thermal stability. We then introduced intra- and intermolecular i-motifs formed by DNAs containing two C-tracts into single-stranded regions within otherwise double-stranded DNA nanocircles. By adjusting the length of C-tracts we can control the intra- and intermolecular folding of i-motif DNAs and achieve programmable functionalization of dsDNA nanocircles. Single-stranded gaps in the nanocircle that are functionalized with an intramolecular i-motif enable the reversible contraction and extension of the DNA circle, as monitored by fluorescence quenching. Thereby, the nanocircle behaves as a proton-fueled DNA prototype machine. In contrast, nanorings containing intermolecular i-motifs induce the assembly of defined multicomponent DNA architectures in response to proton-triggered predicted structural changes, such as dimerization, "kiss", and cyclization. The resulting DNA nanostructures are verified by gel electrophoresis and visualized by atomic force microscopy, including different folding topologies of an intermolecular i-motif. The i-motif-functionalized DNA nanocircles may serve as a versatile tool for the formation of larger interlocked dsDNA nanostructures, like rotaxanes and catenanes, to achieve diverse mechanical operations.
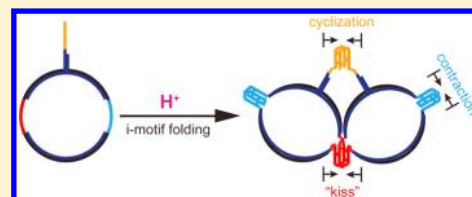
INTRODUCTION

DNA molecules have been extensively used as versatile building materials to construct diverse novel DNA nanostructures,[1] including 2D/3D architectures[2] and interlocked components.[3] The DNA nanostructures can be endowed with programmable functionalities,[4] using proteins,[4b,c] aptamers,[5] DNAzymes,[6] or light-switching molecules.[3b,7] Multistranded DNA motifs, such as G-quadruplexes and i-motifs, have also been employed for structural and functional DNA nanotechnology.[8] Both of these four-stranded motifs share a common feature, namely that their folding patterns usually vary with the sequences or external conditions, which makes it possible in principle to use them as versatile functional tools in DNA nanostructures.

Intramolecular G-quadruplexes and i-motifs have been studied extensively.[9] Their folding is generally accompanied by a change of the size and conformation.[8e−j,10] Bimolecular G-quadruplexes are usually formed by DNAs that contain two G-tracts,[11] but these G-rich DNAs also form larger superstructures called G-wires.[12] Likewise, C-rich DNA sequences can fold into different types of DNA i-motif structures[13] (Figure 1a). Although intramolecular i-motifs have found applications in DNA nanotechnology,[8f,g,j,10b] the intermolecular i-motifs have not yet been employed in this field. Of particular interest is the folding of i-motif DNAs with two C-tracts. These C-rich DNAs can fold into bimolecular,[13b,14] tetramolecular,[13c] or even, as we show here, unimolecular i-motif structures (Figure 1b). A systematic understanding of the conditions that not only direct the folding patterns of these i-motif DNAs but also the

formation of intramolecular versus intermolecular i-motifs will be useful for designing new DNA topologies.

Herein, we systematically study the folding of different i-motif DNAs with two C-tracts that vary in length (Figure 1b, top panel) by polyacrylamide gel electrophoresis (PAGE), circular dichroism (CD), and thermal denaturation. We find that by selecting the appropriate length of C-tracts, the formation of intra- and intermolecular i-motifs can be predicted and controlled (Figure 1b). Based on these findings, we employed these i-motif DNAs to modify a synthetic DNA nanostructure, endowing it with functionalities that can be programmed by means of intra- versus intermolecular i-motif formation. These structural motifs respond to pH change in different ways and form well-defined DNA nanoaggregates that we verify by gel electrophoresis and high-resolution atomic force microscopy (AFM).

RESULTS AND DISCUSSION

Intra- and Intermolecular I-Motif DNAs with Two C-Tracts. We first studied the formation of stable inter- and intramolecular i-motifs. Compared to intramolecular DNA i-motifs,[15] the intermolecular ones reported so far usually have a relatively low stability,[14,16] which has limited their applications in DNA nanotechnology. Therefore, here we aimed at identifying stable bimolecular i-motifs suitable for being
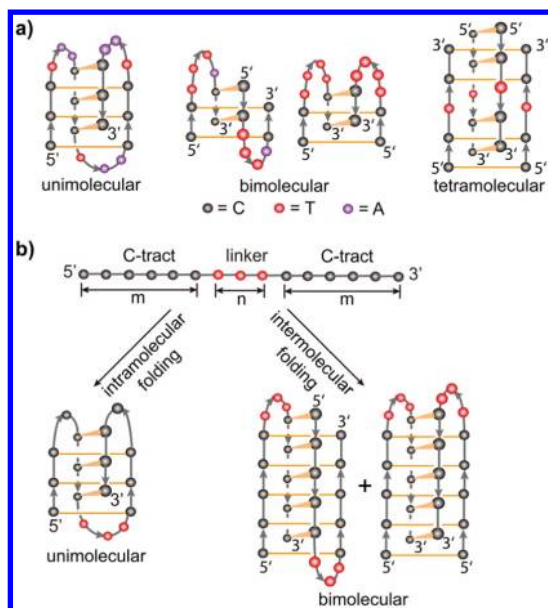
Figure 1. Different types of DNA i-motif structures. (a) Left: Unimolecular i-motif formed by the sequence d[CCC(TAACCC)$_3$]. This i-motif can in principle exist in four different configurations.[13a] Middle: Two different bimolecular i-motifs formed by d(5-methyl-CCTTTACC) and d(5-methyl-CCTTTTCC), respectively.[13b] Right: Tetramolecular i-motif formed by d(5-methyl-CCTCC).[13c] (b) Possible folding patterns of i-motif DNAs with two long C-tracts studied here. Left: A simplified representation for unimolecular i-motifs. Right: A simplified representation for two isomers of bimolecular i-motifs. In these i-motif structures, the number of C·C$^+$ base pairs and loop residues vary as the values of m and n are changed.
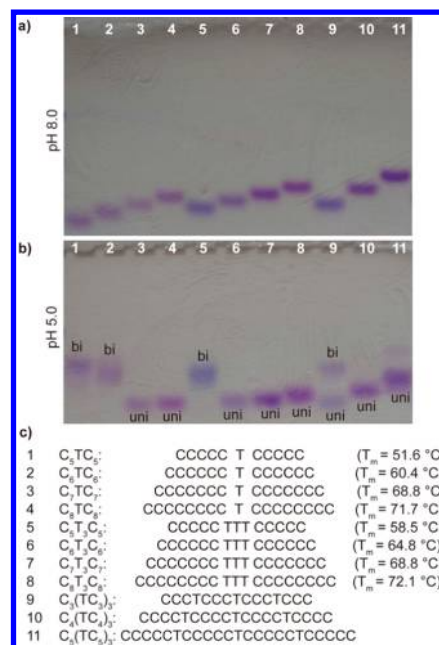

Figure 2. Migration behavior of oligodeoxynucleotidees (ODNs) at acidic and nonacidic pH. Electrophoretograms of 0.2 nmol ODNs in 18% native polyacrylamide gels under different conditions: (a) Migration behavior in 40 mM Tris-AcOH, pH 8.0. Only one band exists in all lanes with the mobility dependent on the molecular weight of single strand, indicating no secondary structure formed in each case. (b) Migration behavior in 40 mM Tris-AcOH, pH 5.0; bi: bimolecular i-motif structure (lanes 1, 2, 5, 9 and 11); and uni: unimolecular i-motif structure. (c) Sequences of the C-rich DNAs and their thermal stability (T_m) at pH 5.0.
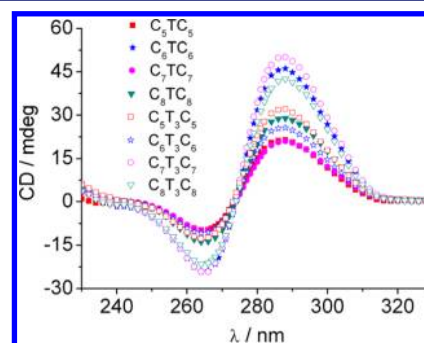
employed as construction components in large DNA architectures. A C-rich DNA with two stretches of cytosines can potentially fold into a bimolecular i-motif,[9b] but two short C-tracts (≤4, e.g., C$_3$TAAC$_3$ and C$_4$ACAC$_4$; see Figure S1a)[16] do not favor the formation of intermolecular i-motifs that remain stably folded at 37 °C. We thus primarily tested DNAs with two long C-tracts spaced by a linker (Figure 1b), i.e., C$_m$T$_n$C$_m$ (m = 5−8, n = 1, 3).

We employed PAGE under nondenaturing conditions to analyze the structures formed by these C-rich DNAs at pH 8.0 and 5.0, respectively (Figure 2). At pH 8.0 only a single band appears for each DNA and displays an electrophoretic mobility primarily dependent on the molecular weight (Figure 2a, lanes 1−11), indicating that each DNA is unfolded. Upon lowering the pH to 5.0, some dramatic changes are observed in the electrophoretic mobility of these DNAs (Figure 2b, lanes 1−11). Their mobility does not entirely depend on molecular weight. The bands of C$_5$TC$_5$, C$_6$TC$_6$, and C$_5$T$_3$C$_5$ have a lower mobility (lanes 1, 2, and 5), whereas the bigger molecules C$_7$TC$_7$, C$_8$TC$_8$, C$_6$T$_3$C$_6$, C$_7$T$_3$C$_7$, and C$_8$T$_3$C$_8$ move fast (lanes 3, 4, 6−8). This is attributed to the formation of i-motif structures, evidenced by CD spectroscopy (Figure 3). All of these DNAs display a dominant positive band near 290 nm and a negative one around 265 nm in the corresponding CD spectra, consistent with the characteristics of i-motif structures.[17] Thermal denaturation shows that the T_m value of folded C$_6$TC$_6$ is increased as the strand concentration increases (see Figure S1b), which is the typical characteristics of the intermolecular structure,[18] indicating that C$_6$TC$_6$ folds into an intermolecular i-motif. In contrast, the T_m value of folded C$_8$TC$_8$ is almost independent of the concentration (Figure

Figure 3. CD spectra of C-rich DNAs (7.5 μM) in 40 mM, pH 5.0 Tris-AcOH buffer. In each case, the CD spectral characteristics of a dominant positive band around 290 nm and a negative one near 265 nm shows the formation of corresponding i-motif structures.

S1c), indicating that it adopts an intramolecular i-motif structure.[18] Based on these data, we conclude that the folded C$_5$TC$_5$ and C$_5$T$_3$C$_5$ behave similar to C$_6$TC$_6$, namely, these two DNAs also form intermolecular i-motifs. Similarly, C$_7$TC$_7$, C$_6$T$_3$C$_6$, C$_7$T$_3$C$_7$, and C$_8$T$_3$C$_8$ all fold into intramolecular i-motifs, just like C$_8$TC$_8$.

As the length of C-tracts increases (i.e., C$_{5\to8}$TC$_{5\to8}$, C$_{5\to8}$T$_3$C$_{5\to8}$), the thermal stability of these i-motifs is improved (see Figure S1d). This is conceivable because longer C-tracts allow more C·C$^+$ base pairs to be formed and to participate in the i-motif core structure, contributing to an increase in stability. However, we always observe a difference between the thermal stability of C$_m$TC$_m$ and C$_m$T$_3$C$_m$, indicating that the length of the linker also has an influence
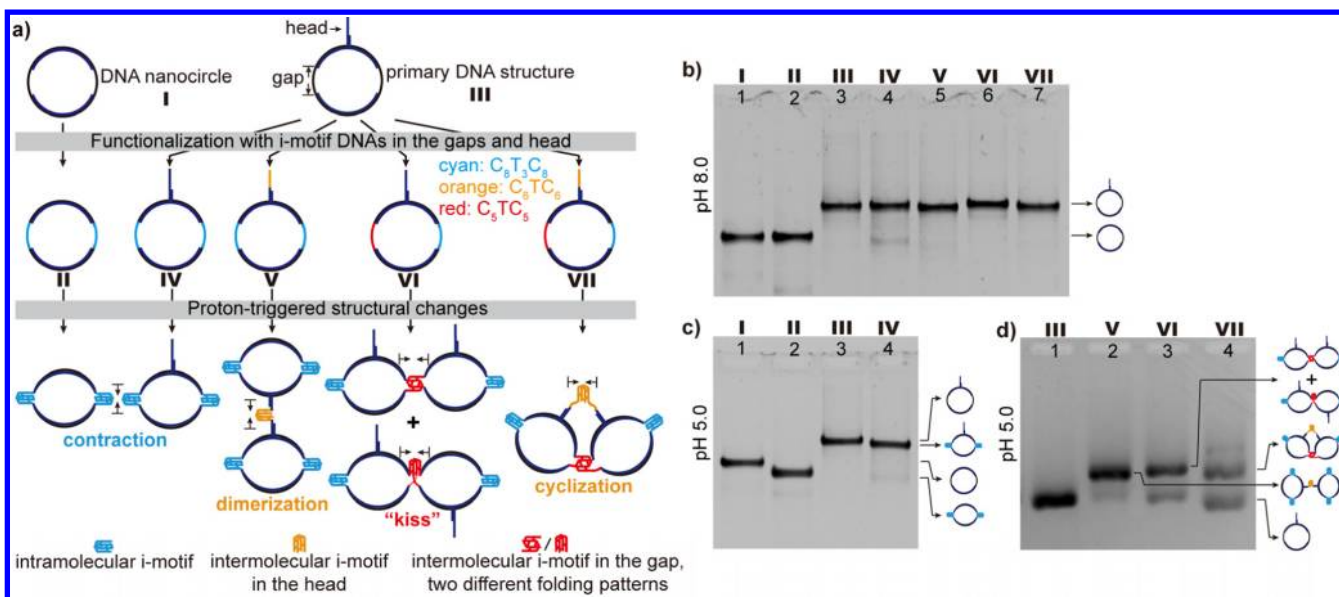
Figure 4. Functionalization of DNA nanocircle with i-motif DNAs. (a) Schematic for the programmable functionalization of DNA nanocircles with intra- and/or intermolecular i-motif DNAs and their expected structural changes triggered by H^+. The designed primary DNA structure (top panel) has two single-stranded gaps in a dsDNA nanocircle. It also contains a flanking duplex with a single stranded overhang (head). These single-stranded regions were functionalized with an unimolecular i-motif $C_8T_3C_8$ (cyan) and two bimolecular i-motifs C_5TC_5 (red) and C_6TC_6 (orange) (middle panel). The folding of these intra- and intermolecular i-motifs enables the DNA structure to respond to pH change and accomplish the programmed structural changes including contraction, dimerization, "kiss", and cyclization (bottom panel). (b) Electrophoretograms of 1.6 pmol DNA nanostructures I–VII (320 nM) in 6% native polyacrylamide gels in 40 mM, pH 8.0 Tris-AcOH buffer. Only one band exists in all lanes, corresponding to the synthesized DNA nanostructures shown in (a), top panel. (c) Electrophoretograms of DNA nanostructures I–IV in 40 mM, pH 5.0 Tris-AcOH buffer. An observable shift in the mobility of bands originates from the contraction of two gaps of DNA nanostructures (lanes 2, 4 vs lanes 1, 3). (d) Electrophoretic analysis of the H^+-induced assemblies of DNA nanostructures V–VII in 2% agarose gel; reference: III (lane 1). The new bands correspond to the indicated DNA nanostructures.

on the i-motif structures.[15b] Note that both C_6TC_6 and $C_5T_3C_5$ have a widened band with a similar electrophoretic mobility (Figure 2b, lanes 2, 5). These two intermolecular i-motifs also have a similar thermal stability under the same conditions (see Figure S1d). In contrast, the stability of C_5TC_5 is lower than that of $C_5T_3C_5$. More remarkable differences are observed between C_6TC_6 and $C_6T_3C_6$. The former folds into an intermolecular i-motif (Figure 2b, lane 2), whereas the latter adopts a more stable intramolecular structure (Figure 2b, lane 6). These observations strongly suggest that the single-T linker of C_5TC_5 and C_6TC_6 is not enough to span the groove of the corresponding i-motif structure, and so it cannot serve as the loop unless together with some (one or more) nearby C residues. Thus, some C residues of C_5TC_5 and C_6TC_6 are not engaged in the i-motif core structure but are part of the loop of the resulting i-motifs. As a consequence, C_5TC_5 and C_6TC_6 cannot form the same i-motif core structures as $C_5T_3C_5$ and $C_6T_3C_6$, respectively. These findings are consistent with previous observations that $C_2T_4C_2$ folds into a bimolecular i-motif with two T_4 loops,[13b] whereas C_2TC_2 only forms a tetramolecular i-motif structure.[13c]

Since some i-motif DNAs consisting of four C-tracts and three single-residue linkers should also be able to form bimolecular i-motifs,[15b,19] we included this group of C-rich DNAs (i.e., $C_m(TC_m)_3$, $m = 3–5$) in our PAGE analysis (Figure 2, lanes 9–11). Although $C_2(TC_2)_3$ is reported to fold into a bimolecular i-motif under acidic conditions,[15b] $C_3(TC_3)_3$ forms an almost 1:1 mixture of unimolecular and bimolecular species (Figure 2b, lane 9). As the length of C-tracts increases, the unimolecular species become dominant (lanes 10, 11).

These observations clearly demonstrate an important influence of the length of C-tracts and spacer length on the inter- versus intramolecular folding of i-motifs. For those i-motif DNAs with two stretches of six or less C-residues, the intermolecular folding is favored. In contrast, longer C-tracts (≥ 7) allow these DNAs to form intramolecular i-motifs, independent of the sequence and length of the linker (see Figure S2).

Under the conditions employed here, C_6TC_6 exhibits the highest thermal stability among the bimolecular i-motifs known to date ($T_m = 60.4\ °C$). Similarly, the intramolecular i-motif DNAs with two longer C-tracts also display unusually high thermal stability. For example, the T_m value of $C_8T_3C_8$ reaches to over 70 °C, higher than that of a well-known i-motif[13a] formed by human telomeric DNA ($(C_3TAA)_3C_3$) with a T_m of ~60 °C under very similar conditions. The high stability of the intramolecular i-motif $C_8T_3C_8$ and its possible folding patterns are discussed in Figure S3.

DNA Nanocircles with Programmable Functionalities. Based on the insight into the conditions that determine the intra- versus intermolecular folding of these i-motif DNAs, we next sought to employ them for the controlled functionalization of a double-stranded DNA nanocircle[20] (Figure 4a). Two single-stranded gap regions are symmetrically located on opposing sides of the DNA nanocircle, that can be functionalized at will with different oligodeoxynucleotide (ODN) sequences.[21] Thereby, the nanocircles can serve as versatile construction components that can be incorporated, for example, into interlocked DNA nanoarchitectures, such as catenanes[3c,d] and rotaxanes.[3a,b,22] In addition, the DNA
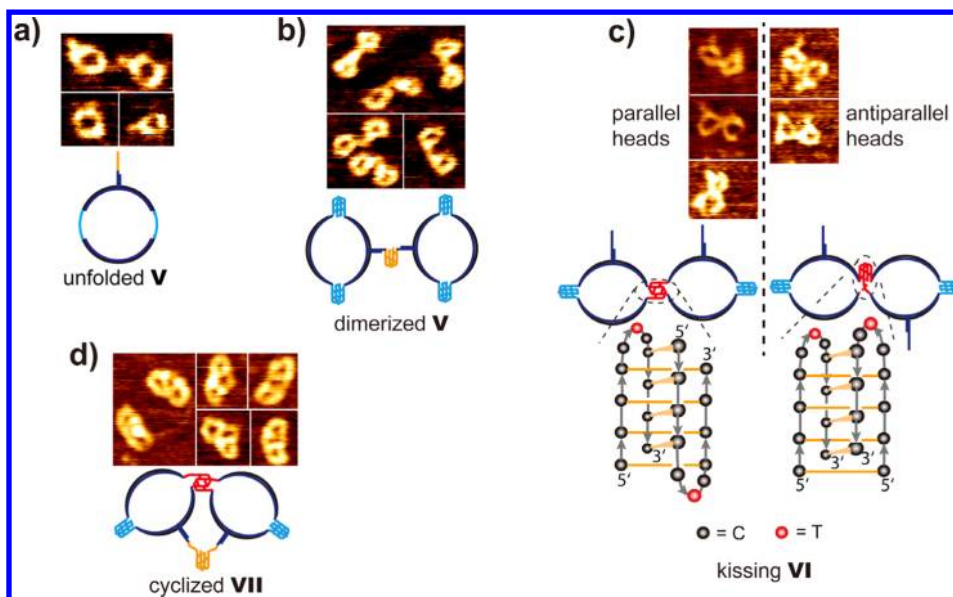
Figure 5. AFM confirmation of the formation of DNA nanostructures illustrated in Figure 4. (a) AFM image of the DNA structure V at pH 8.0, with two clearly observed gaps and one head. (b) AFM image of the DNA structure V at pH 5.0, indicating the formation of a head-to-head dimer. (c) AFM images of the DNA structure VI at pH 5.0, demonstrating that two monomers are kissing in either a parallel or an antiparallel manner. It originates from two different folding patterns of the bimolecular i-motif C_5TC_5, as illustrated in the bottom panel. (d) AFM images of the DNA structure VII at pH 5.0, showing the cyclization on two heads of a parallel dimer. The entire AFM images of (a−d) are provided in Figure S6.

nanocircles contain a single-stranded branch tethered to a duplex flanking the circle. This motif is hereafter called "head".

The various i-motif sequences are located within the single-stranded gaps and head, allowing the DNA architecture to variably respond to pH change. Due to their structural robustness, C_6TC_6 and $C_8T_3C_8$ appeared to be good candidates for intra- and intermolecular i-motif DNAs, respectively, used in our system. However, the presence of the C_6TC_6 sequence in both the gap and head would result in an unwanted and uncontrollable interaction between these sites during the pH-induced formation of the bimolecular i-motifs. Therefore, to prevent the undesired interaction between head and gap motifs, one of the sites needs to be equipped with a bimolecular i-motif that displays a faster folding kinetics than the other one. As a candidate motif, we placed C_5TC_5 in the gap and C_6TC_6 in the head. C_5TC_5 is less stable than C_6TC_6, but it folds with faster kinetics (see Figure S4), so that bimolecular i-motif formation should occur in a two-step cyclization process, in which the gaps of DNA nanostructure fold in advance of the head.

Functionalizing the primary DNA structure III (that cannot form an i-motif) and the reference circle I (Figure 4a, top panel) with i-motif DNAs will result in the corresponding functional structures IV−VII and II (Figure 4a, middle panel). Due to the intra- and intermolecular folding of i-motif DNAs on their head and in the gaps, these structures are expected to undergo the H⁺-triggered structural changes shown in Figure 4a (bottom panel). To test these possibilities, we synthesized these DNA structures (see Supporting Information) and then analyzed the electrophoretic behavior of different DNA structures by native PAGE and agarose gel electrophoresis (Figure 4b−d). At pH 8.0, the structures IV−VII all have just one band in the gel with an electrophoretic mobility similar to that of III (Figure 4b, lanes 3−7). This indicates that the C-rich gaps and head of IV−VII are unfolded, as verified by AFM (Figure 5a). The head and two gaps of the DNA structure V are observed clearly at pH 8.0.

Upon lowering the pH to 5.0, some dramatic changes are observed in the electrophoretic behavior of different DNA structures (Figure 4c,d). There is a slight increase in the electrophoretic mobility of IV (Figure 4c, lane 4), as compared with the reference III (lane 3). The H⁺-induced shift in the electrophoretic mobility of DNA circle II can be observed more clearly (lane 2 vs lane 1).

These pH-induced changes of the mobility of IV and II are consistent with the proposed intramolecular i-motif folding of C_8TC_8 in their gaps, as indicated in Figure 4c. In general, the folding of intramolecular i-motifs is accompanied by a slight reduction in the size due to ring contraction[8f] that increases the electrophoretic mobility. This contraction is too faint to be observable by AFM (Figure 5a vs b−d). Therefore, to prove that the H⁺-induced contraction in the architectures containing nanocircles of type II or V does occur, we performed a fluorescence quenching (FQ) study using the type II circles as a model.

Since the two gaps in the type II circles are both functionalized with the same i-motif, only one of them was monitored. We labeled its two terminals with carboxytetramethyl rhodamine (TAMRA) and a quencher (BHQ-2). This resulted in a reversible FQ system in which the H⁺-driven contraction and extension of the gap can be monitored (Figure 6a). As a control, the reference circle I without the ability to form an i-motif was labeled in the same way and monitored in parallel. TAMRA can work in a wide pH range, as its fluorescence is insensitive to pH change (see Figure S7), similar to Rhodamine Green.[8f,10b,23] At pH 8, the i-motif DNA is unfolded, and the gap is extended. In this case, the dye and quencher are separate, and no FQ occurs. Indeed, a bright fluorescence is observed in this system (Figure 6b). Adjusting the pH to 5.0 resulted in a sharp decrease in the fluorescence intensity (Figure 6c, black bars, FQ). In contrast, the reference circle I only shows a small fluorescence decrease (Figure 6c, control, gray bars) that is mainly due to the slight (<20%) decrease of TAMRA fluorescence emission under acidic
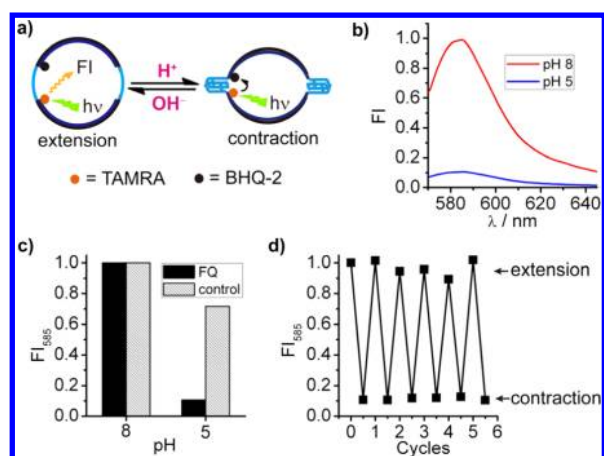
Figure 6. (a) Schematic for the working principle of a fluorescence quenching (FQ) system built on the contraction/extension of the gaps of the DNA circle II. (b) Fluorescence spectra of the FQ system at different pH. Excitation wavelength: 550 nm. The fluorescence intensity was normalized. (c) Control experiment for the FQ system. The reference DNA circle I of which one gap was also labeled with TAMRA and BHQ-2 was used as the control. The fluorescence intensity was always monitored at 585 nm (FI_{585}) and normalized. (d) Working cycles of the FQ system switched between pH 8 and 5 are consistent with the extension and contraction of the gaps.

conditions (see Figure S7). This demonstrates that the fluorescence change in the type II circle results from an efficient FQ between TAMRA and BHQ-2 in the closed state,[24] corresponding to the gap contraction of the DNA circle induced by the folding into the intramolecular i-motif DNA at pH 5.0. The contracted gaps of the DNA nanocircle can be reset to the extended state at pH 8 and can be further switched many times in a fully reversible fashion (Figure 6d).[8f,g,10b,23,25] In this way, the DNA structure II behaves as a prototype machine that can be switched back and forth between a contracted and expanded state.

In contrast to the intramolecular i-motif (C_8TC_8), the folding of bimolecular DNA i-motifs (C_6TC_6 and C_5TC_5) in the gaps and head of the DNA structures V−VII results in a H^+-dependent assembly of DNA structures that markedly differs from that of III. This is reflected by the appearance of new slowly moving bands in 2% agarose gel (Figure 4d, lanes 2−4), while the bands corresponding to the monomeric structures become markedly reduced (compare with lane 1). We employed agarose gel electrophoresis to analyze V−VII at pH 5.0 (Figure 4d), because the formed larger DNA nano-architectures move too slowly in PAGE.

The unusual stability of the bimolecular i-motif C_6TC_6 enables most of V to form a head-to-head dumbbell-shaped dimer (Figure 4d, lane 2), as verified by AFM (Figure 5b).[8c,26] C_5TC_5 dimerizes in a gap−gap interaction in which one gap of VI interacts with a gap in another molecule of VI by forming a bimolecular i-motif. This interaction enables this DNA structure (Figure 4d, lane 3) to form two kinds of dimers: As evident from the corresponding AFM image (Figure 5c), two monomers can either dimerize in a parallel manner that results in a face-to-face kissing interaction with two heads on the same side (Figure 5c, left panel) or in an antiparallel manner with two heads on opposite sides (Figure 5c, right panel). The formation of parallel and antiparallel dimers results from two different folding patterns of a bimolecular i-motif (Figure 1),[15b] as illustrated in Figure 5c. As the 5′ and 3′ termini of C_5TC_5 are

both fixed in the DNA nanocircle, different arrangements of these two terminals in the i-motif structure induce the two kissing circles to turn on the same or opposite directions. By this means, these i-motif folding patterns are for the first time indirectly visualized by AFM. In this way, the bimolecular i-motif kissing interactions differ from "kissing-loop" structures requiring RNA hairpins.[27] Although the unimolecular i-motif in another gap does not participate in the kissing interaction, it might help contracting the gap, which would promote the formation of the kissing dimers to some extent (see Figure S5b).

The DNA structure VII carries both C_6TC_6 and C_5TC_5 in the head and gap, respectively. Its assembly is built on the difference between the folding kinetics of C_6TC_6 and C_5TC_5 (see Figure S4). Under identical conditions, the folding of C_5TC_5 into the i-motif structure is faster than C_6TC_6, reflected by a higher folding kinetic rate[28] (Figure S4, insert). Therefore, the DNA structure VII should first dimerize into the "kissing" structure (see Figure 5c) rather than via its head-groups (see Figure 5b). As a consequence, VII is expected to undergo a two-step assembly under acidic conditions. First, parallel and antiparallel dimers are formed via the folding of C_5TC_5 in the gap. Subsequently, the intermolecular folding of C_6TC_6 on the heads of a parallel dimer connects two heads together, leading to further cyclization. The formed dimer resembles a three-ring structure, as shown in the corresponding AFM image (Figure 5d). The resulting rigidity of this type of dimer slightly increases the electrophoretic mobility (Figure 4d, lane 4), as compared to the dimers formed by VI that cannot engage in further cyclization (see Figure 4d, lane 3).

The two heads in the antiparallel dimer of VII cannot cyclize for steric reasons. Instead, the bimolecular i-motif C_6TC_6 in the head can potentially induce further aggregation into larger structures. In this case the dimer is in principle able to interact with one or two free monomers to form a trimer or tetramer. In contrast to the intrastructural cyclization, the formation of trimers or tetramers in the second step is an interstructural interaction that is highly dependent on the concentration of the DNA structure VII. Under the conditions employed here, the trimer and tetramer rarely form, as indicated in Figure 4d (lane 4). At higher concentrations, however, the bands corresponding to the trimer and tetramer are clearly observed in agarose gel electrophoresis, while the band corresponding to the monomer almost disappears (see Figure S8). This concentration-dependent feature makes it difficult to visualize the trimer and tetramer structures by AFM because the DNA solutions become too concentrated to yield meaningful AFM images (see Experimental Section). On the other hand, this feature may become useful in the context of larger interlocked dsDNA nanostructures, like rotaxanes[3a,b,22] or catenanes.[3c,d] In this case, interlocked DNA nanocircles functionalized with bimolecular i-motifs are expected to undergo pH-triggered intrastructural assemblies. The undesired interstructural interactions between two or more molecules of rotaxanes or catenanes would be avoided by DNA concentration control.

■ CONCLUSIONS

We have systematically studied the intra- and intermolecular folding of i-motif DNAs with two C-tracts, revealing an influence of the length of their C-tracts on the intra- versus intermolecular i-motif structures. Two stretches of six or less C-residues, such as C_6TC_6 and C_5TC_5, favor the intermolecular folding of i-motifs, whereas longer C-tracts (e.g., $C_8T_3C_8$)

promote the formation of intramolecular i-motif structures with unusually high thermal stability, demonstrated by PAGE, CD, and thermal denaturation.

We have employed the various intra- and intermolecular i-motif DNAs for the functionalization of single-stranded 'gap' regions and a branched-out 'head' structure of double-stranded DNA nanocircles. The intra- and intermolecular folding of these i-motif DNAs can be used to alter the DNA structure in response to pH change. The structural changes we observed under acidic conditions include nanocircle contraction, dimerization, kiss, and cyclization. We verified the resulting nanostructures by gel electrophoresis and AFM. By this means, two different folding patterns of a bimolecular i-motif could be visualized. In addition, we have employed a DNA nanocircle modified with a gap sequence containing an intramolecular i-motif to operate a pH-driven DNA nanoarchitecture that can be regarded as a prototype of a circular contraction/expansion device.

Our study provides insight into the controllable intra- versus intermolecular folding of i-motif DNAs and demonstrates how to harness this knowledge for the functional programming of DNA nanocircles. It will open new ways to operate larger interlocked DNA nanoarchitectures and nanomachines, like dsDNA rotaxanes[3a,b,22] or catenanes,[3c,d] where the mobility of i-motif-modified DNA nanocircles in these structures will be driven by pH in a highly reversible fashion. The bimolecular i-motifs in the gap and head of DNA nanocircles can serve as anchors for controlling mechanical motion of interlocked macrocycles, for programming the dynamic topologies of the interlocked systems,[3d] or for operating individual components in DNA nanomechanics.

■ EXPERIMENTAL SECTION

I-Motif DNAs. HPLC-purified and MS-verified C-rich DNAs were obtained from METABION (Martinsried, Germany) and quantified by using a multimode microplate reader (Tecan Austria GmbH). Each DNA (20 μM) was incubated at 87 °C for 10 min in 40 mM Tris-AcOH buffer (pH 5.0), then slowly cooled to 4 °C and incubated overnight, allowing C-rich DNAs to properly fold into the i-motif structures. As the control, these sequences were meanwhile incubated at pH 8.0 under the same conditions.

Gel Electrophoresis. Nondenaturing polyacrylamide gel (18%) was used for i-motif DNAs and prepared in 40 mM, pH 8.0/5.0 Tris-AcOH buffer. Gel electrophoresis was run in the same buffer at 4 °C for 16 h under a voltage of 4 V/cm. The gel was then stained in 0.01% Stains-All solution and destained under light, finally photographed with a camera. 6% nondenaturing polyacrylamide gel was used for DNA nanocircles. In this case, gel electrophoresis was run at room temperature under 4 V/cm for 4 h. The gel was then stained by GelRed and photographed under UV light. 2% agarose gel was used for the electrophoretic analysis of the assemblies of DNA nanocircles. Gel electrophoresis was run at room temperature under 4 V/cm for 3 h. The gel was then photographed using GelRed staining.

CD Measurements. The CD spectra of 7.5 μM C-rich DNAs in pH 5.0, 40 mM Tris-AcOH buffer were collected at room temperature with a JASCO J-810 spectropolarimeter (Tokyo, Japan). The optical chamber (5 mm path length, 1200 μL) was deoxygenated with dry purified nitrogen before use and the nitrogen atmosphere was kept during experiments. Three scans from 230 to 330 nm were accumulated and averaged. In each case, the background of the buffer solution was subtracted from the CD data.

Melting Curves. The melting curves of 5 μM DNA i-motifs at pH 5.0 in 40 mM Tris-AcOH buffer were monitored at 295 nm by a UV spectrometer equipped with a temperature controlled water bath, with a rate of 0.2 °C/min. The absorbance at 295 nm (A_{295}) was

normalized in each case. The T_m value of i-motifs was obtained, at which 50% of i-motif structures were dissociated.

DNA Nanocircles. The designed primary DNA structure has two C-rich single-stranded gaps in a double-stranded nanocircle and a duplex head with one C-rich single-stranded terminal. Eight component sequences were first incubated at 60 °C for 2 min, then slowly cooled to 15 °C. The ligation was performed overnight in the presence of T4 DNA ligase and the ligation buffer (40 mM Tris-HCl, 10 mM MgCl$_2$, 10 mM DTT, 0.5 mM ATP, pH 7.8), followed by HPLC purification. The synthesized DNA nanostructure (320 nM) was incubated at 37 °C for 5 h at pH 5.0 and slowly cooled to 4 °C, allowing their C-rich regions to properly fold into the i-motif structures.

Fluorescence Quenching (FQ). The dye/quencher-labeled i-motif sequences in the gap region of DNA nanocircles was synthesized, purified, and then prepared in pH 8, 40 mM Tris-AcOH buffer at a working concentration of 0.5 μM. The pH value of this FQ system was switched between pH 8.0 and 5.0 by alternate addition of 1% (v/v) of 3 M HCl and 3 M NaOH. After each pH switch, the system was incubated at 60 °C for 30 min, allowing the i-motif DNA in the gaps of the circle to properly fold. Subsequently, the sample is cooled slowly to room temperature for fluorimetry. The fluorescence change was recorded by an EnSpire multimode plate reader (PerkinElmer).

AFM. The formation of DNA nanostructures was confirmed by AFM: Nanowizard 3, JPK Instruments; measuring modes: AC in air; substrate: mica with linear polyethylene imine. Just before measurements, the above-prepared sample was diluted to 6 nM with 40 mM Tris-AcOH (pH 4.5) containing 12.5 mM MgCl$_2$ and 2.5 mM EDTA.

■ ASSOCIATED CONTENT

Ⓢ Supporting Information

Figures S1−S8 and discussions; Table S1 and the details of the synthesized DNA nanostructures. This material is available free of charge via the Internet at http://pubs.acs.org.

■ AUTHOR INFORMATION

Corresponding Author
*Corresponding Author m.famulok@uni-bonn.de

Notes
The authors declare no competing financial interest.

■ ACKNOWLEDGMENTS

■ REFERENCES

(1) (a) Seeman, N. C. *Annu. Rev. Biochem.* **2010**, *79*, 65. (b) Feldkamp, U.; Niemeyer, C. M. *Angew. Chem., Int. Ed.* **2006**, *45*, 1856. (c) Simmel, F. C. *Angew. Chem., Int. Ed.* **2008**, *47*, 5884. (d) McLaughlin, C. K.; Hamblin, G. D.; Sleiman, H. F. *Chem. Soc. Rev.* **2011**, *40*, 5647. (e) Pinheiro, A. V.; Han, D.; Shih, W. M.; Yan, H. *Nat. Nanotechnol.* **2011**, *6*, 763.

(2) (a) Kallenbach, N. R.; Ma, R. I.; Seeman, N. C. *Nature* **1983**, *305*, 829. (b) Rothemund, P. W. *Nature* **2006**, *440*, 297. (c) Han, D.; Pal, S.; Nangreave, J.; Deng, Z.; Liu, Y.; Yan, H. *Science* **2011**, *332*, 342. (d) Andersen, E. S.; Dong, M.; Nielsen, M. M.; Jahn, K.; Subramani, R.; Mamdouh, W.; Golas, M. M.; Sander, B.; Stark, H.; Oliveira, C. L.; Pedersen, J. S.; Birkedal, V.; Besenbacher, F.; Gothelf, K. V.; Kjems, J. *Nature* **2009**, *459*, 73. (e) Goodman, R. P.; Heilemannt, M.; Dooset, S.; Erben, C. M.; Kapanidis, A. N.; Turberfield, A. J. *Nat. Nanotechnol.* **2008**, *3*, 93.

(3) (a) Ackermann, D.; Schmidt, T. L.; Hannam, J. S.; Purohit, C. S.; Heckel, A.; Famulok, M. *Nat. Nanotechnol.* **2010**, *5*, 436. (b) Lohmann, F.; Ackermann, D.; Famulok, M. *J. Am. Chem. Soc.* **2012**, *134*, 11884.

(c) Schmidt, T. L.; Heckel, A. *Nano Lett.* **2011**, *11*, 1739. (d) Elbaz, J.; Wang, Z. G.; Wang, F.; Willner, I. *Angew. Chem., Int. Ed.* **2012**, *51*, 2349.

(4) (a) Wilner, O. I.; Willner, I. *Chem. Rev.* **2012**, *112*, 2528. (b) Sacca, B.; Niemeyer, C. M. *Chem. Soc. Rev.* **2011**, *40*, 5910. (c) Teller, C.; Willner, I. *Trends Biotechnol.* **2010**, *28*, 619.

(5) (a) Rinker, S.; Ke, Y.; Liu, Y.; Chhabra, R.; Yan, H. *Nat. Nanotechnol.* **2008**, *3*, 418. (b) Chhabra, R.; Sharma, J.; Ke, Y.; Liu, Y.; Rinker, S.; Lindsay, S.; Yan, H. *J. Am. Chem. Soc.* **2007**, *129*, 10304. (c) Douglas, S. M.; Bachelet, I.; Church, G. M. *Science* **2012**, *335*, 831.

(6) (a) Willner, I.; Shlyahovsky, B.; Zayats, M.; Willner, B. *Chem. Soc. Rev.* **2008**, *37*, 1153. (b) Lund, K.; Manzo, A. J.; Dabby, N.; Michelotti, N.; Johnson-Buck, A.; Nangreave, J.; Taylor, S.; Pei, R. J.; Stojanovic, M. N.; Walter, N. G.; Winfree, E.; Yan, H. *Nature* **2010**, *465*, 206. (c) Elbaz, J.; Lioubashevski, O.; Wang, F.; Remacle, F.; Levine, R. D.; Willner, I. *Nat. Nanotechnol.* **2010**, *5*, 417.

(7) (a) Schmidt, T. L.; Koeppel, M. B.; Thevarpadam, J.; Goncalves, D. P.; Heckel, A. *Small* **2011**, *7*, 2163. (b) You, M.; Chen, Y.; Zhang, X.; Liu, H.; Wang, R.; Wang, K.; Williams, K. R.; Tan, W. *Angew. Chem., Int. Ed.* **2012**, *51*, 2457.

(8) (a) Alberti, P.; Bourdoncle, A.; Sacca, B.; Lacroix, L.; Mergny, J. L. *Org. Biomol. Chem.* **2006**, *4*, 3383. (b) Dutta, K.; Fujimoto, T.; Inoue, M.; Miyoshi, D.; Sugimoto, N. *Chem. Commun.* **2010**, *46*, 7772. (c) Goncalves, D. P.; Schmidt, T. L.; Koeppel, M. B.; Heckel, A. *Small* **2010**, *6*, 1347. (d) Sannohe, Y.; Endo, M.; Katsuda, Y.; Hidaka, K.; Sugiyama, H. *J. Am. Chem. Soc.* **2010**, *132*, 16311. (e) Alberti, P.; Mergny, J. L. *Proc. Natl. Acad. Sci. U.S.A.* **2003**, *100*, 1569. (f) Liu, D.; Balasubramanian, S. *Angew. Chem., Int. Ed.* **2003**, *42*, 5734. (g) Shu, W.; Liu, D.; Watari, M.; Riener, C. K.; Strunz, T.; Welland, M. E.; Balasubramanian, S.; McKendry, R. A. *J. Am. Chem. Soc.* **2005**, *127*, 17054. (h) Xu, Y.; Hirao, Y.; Nishimura, Y.; Sugiyama, H. *Bioorg. Med. Chem.* **2007**, *15*, 1275. (i) Elbaz, J.; Wang, Z. G.; Orbach, R.; Willner, I. *Nano Lett.* **2009**, *9*, 4510. (j) Wang, C.; Huang, Z.; Lin, Y.; Ren, J.; Qu, X. *Adv. Mater.* **2010**, *22*, 2792.

(9) (a) Burge, S.; Parkinson, G. N.; Hazel, P.; Todd, A. K.; Neidle, S. *Nucleic Acids Res.* **2006**, *34*, 5402. (b) Gueron, M.; Leroy, J. L. *Curr. Opin. Struct. Biol.* **2000**, *10*, 326.

(10) (a) Dittmer, W. U.; Reuter, A.; Simmel, F. C. *Angew. Chem., Int. Ed.* **2004**, *43*, 3550. (b) Liu, D.; Bruckbauer, A.; Abell, C.; Balasubramanian, S.; Kang, D. J.; Klenerman, D.; Zhou, D. *J. Am. Chem. Soc.* **2006**, *128*, 2067. (c) Mao, Y. D.; Liu, D. S.; Wang, S. T.; Luo, S. N.; Wang, W. X.; Yang, Y. L.; Qi, Q. Y.; Lei, J. *Nucleic Acids Res.* **2007**, *35*, e33. (d) Ge, B.; Huang, Y. C.; Sen, D.; Yu, H. Z. *Angew. Chem., Int. Ed.* **2010**, *49*, 9965.

(11) (a) Schultze, P.; Smith, F. W.; Feigon, J. *Structure* **1994**, *2*, 221. (b) Phan, A. T.; Patel, D. J. *J. Am. Chem. Soc.* **2003**, *125*, 15021. (c) Phan, A. T.; Modi, Y. S.; Patel, D. J. *J. Mol. Biol.* **2004**, *338*, 93.

(12) (a) Marsh, T. C.; Henderson, E. *Biochemistry* **1994**, *33*, 10718. (b) Marsh, T. C.; Vesenka, J.; Henderson, E. *Nucleic Acids Res.* **1995**, *23*, 696.

(13) (a) Leroy, J. L.; Gueron, M.; Mergny, J. L.; Helene, C. *Nucleic Acids Res.* **1994**, *22*, 1600. (b) Nonin, S.; Phan, A. T.; Leroy, J. L. *Structure* **1997**, *5*, 1231. (c) Nonin, S.; Leroy, J. L. *J. Mol. Biol.* **1996**, *261*, 399.

(14) Gallego, J.; Chou, S. H.; Reid, B. R. *J. Mol. Biol.* **1997**, *273*, 840.

(15) (a) Manzini, G.; Yathindra, N.; Xodo, L. E. *Nucleic Acids Res.* **1994**, *22*, 4634. (b) Mergny, J. L.; Lacroix, L.; Han, X. G.; Leroy, J. L.; Helene, C. *J. Am. Chem. Soc.* **1995**, *117*, 8887.

(16) Kaushik, M.; Prasad, M.; Kaushik, S.; Singh, A.; Kukreti, S. *Biopolymers* **2010**, *93*, 150.

(17) Kypr, J.; Kejnovska, I.; Renciuk, D.; Vorlickova, M. *Nucleic Acids Res.* **2009**, *37*, 1713.

(18) Mergny, J. L.; Lacroix, L. *Oligonucleotides* **2003**, *13*, 515.

(19) Li, T.; Ackermann, D.; Hall, A. M.; Famulok, M. *J. Am. Chem. Soc.* **2012**, *134*, 3508.

(20) (a) Ulanovsky, L.; Bodner, M.; Trifonov, E. N.; Choder, M. *Proc. Natl. Acad. Sci. U.S.A.* **1986**, *83*, 862. (b) MacDonald, D.; Herbert, K.; Zhang, X.; Pologruto, T.; Lu, P. *J. Mol. Biol.* **2001**, *306*, 1081.

(21) Rasched, G.; Ackermann, D.; Schmidt, T. L.; Broekmann, P.; Heckel, A.; Famulok, M. *Angew. Chem., Int. Ed.* **2008**, *47*, 967.

(22) Ackermann, D.; Jester, S. S.; Famulok, M. *Angew. Chem., Int. Ed.* **2012**, *51*, 6771.

(23) Liedl, T.; Olapinski, M.; Simmel, F. C. *Angew. Chem., Int. Ed.* **2006**, *45*, 5007.

(24) Marras, S. A.; Kramer, F. R.; Tyagi, S. *Nucleic Acids Res.* **2002**, *30*, e122.

(25) (a) Liedl, T.; Simmel, F. C. *Nano Lett.* **2005**, *5*, 1894. (b) Liu, H. J.; Xu, Y.; Li, F. Y.; Yang, Y.; Wang, W. X.; Song, Y. L.; Liu, D. S. *Angew. Chem., Int. Ed.* **2007**, *46*, 2515.

(26) Ackermann, D.; Rasched, G.; Verma, S.; Schmidt, T. L.; Heckel, A.; Famulok, M. *Chem. Commun.* **2010**, *46*, 4154.

(27) (a) Mayer, G.; Ackermann, D.; Kuhn, N.; Famulok, M. *Angew. Chem., Int. Ed.* **2008**, *47*, 971. (b) Chang, K. Y.; Tinoco, I., Jr. *Proc. Natl. Acad. Sci. U.S.A.* **1994**, *91*, 8705.

(28) Zhao, Y.; Zeng, Z. X.; Kan, Z. Y.; Hao, Y. H.; Tan, Z. *ChemBioChem* **2005**, *6*, 1957.